Korean J. Chem. Eng., 40(9), 2253-2262 (2023)
DOI: 10.1007/s11814-023-1413-3

pISSN: 0256-1115
eISSN: 1975-7220

Removal of free fatty acid from waste cooking oil using an adsorbent derived from cassava peels

Amnat Phetrungnapha†, Nalinnipa Wiengnak, and Kamol Maikrang

Department of Biochemistry, Faculty of Medical Science, Naresuan University, Phitsanulok, Thailand 65000
(*Received 13 December 2022 • Revised 28 February 2023 • Accepted 7 March 2023*)

Abstract−The present study investigated the potential use of the cassava peel-derived adsorbent for removal of free fatty acid (FFA) from waste cooking oil (WCO). The adsorbent A3 was developed by calcination at 200 °C for 2 hours, followed by NaOH modification. The surface morphology and functional groups of A3 were characterized using Fourier transform infrared spectroscopy (FT-IR) and scanning electron microscopy (SEM). Adsorption parameters, such as adsorbent dose, contact time, and temperature, influenced the adsorption efficiency of A3 for FFA. Isotherms, kinetics and thermodynamics of free fatty acid (FFA) adsorption onto A3 were investigated. The maximum adsorption capacity (q_m) of A3 for FFA was 322.58 mg/g at a temperature of 35 °C. Adsorption isotherm was well described by the Freundlich model (R^2=0.9676), while adsorption kinetics was best fitted with pseudo-second order model (R^2=0.9996). Kinetic data revealed that the adsorption of FFA onto A3 was chemisorption. Thermodynamic studies revealed that FFA adsorption was endothermic, favorable, and spontaneous. In addition, diethyl ether and chloroform : methanol (2 : 1, v/v) could be used for chemical regeneration of A3. Our results confirmed that A3 has the potential to be a suitable adsorbent for FFA removal from WCO.

Keywords: Waste Cooking Oil, Free Fatty Acid, Adsorption, Adsorbent, Cassava Peels

INTRODUCTION

The global consumption of cooking oil is 41-67 million metric tons per year, and waste cooking oil (WCO) production is estimated to be 20-32% of the total consumption [1]. WCO is mainly produced by households, hospitality sectors, and the food industry and is considered one of the hazards to the environment and human health. Improper disposal of WCO leads to various cascading problems, such as sewage clogs, wastewater overflow, costly damage to infrastructure, vectors and pests, nauseous odors, and higher operating costs at central wastewater treatment plants [2]. A proper WCO management system and circular economy can help to minimize socio-economic and environmental problems.

WCO can be the best feedstock choice for biodiesel, hydrogen gas, and low molecular weight hydrocarbons as the amount of its production becomes larger [3-5]. Various chemical reactions, such as hydrolysis, oxidation, and polymerization, occur during the deep-frying process. Volatile compounds, free fatty acids, lipid peroxides, hydrocarbons, and polymers are produced in cooking oil [6]. Typically, biodiesel production comprises the process of transesterification, where a triglyceride reacts with an alcohol to form esters and glycerol. The reaction occurs in the presence of a catalyst, usually a strong alkaline like sodium hydroxide [7]. The initial FFA content in raw materials significantly affects alkali-catalyzed transesterification. A large amount of FFA in the reaction can lead to soap formation, low production yield, and complicated downstream and recovery processes [8]. Two-step processes have been developed for biodiesel production to solve this problem. In the first step, FFA are esterified and catalyzed by acid as a pre-treatment. The second step is the transesterification of the glycerides using a homogeneous alkali catalyst. However, the first step is time-consuming and requires large amounts of methanol and acid catalyst [9,10]. In addition, supercritical transesterification and enzymatic catalysis have been used for pre-treatment of WCO with high FFA content, but these methods are expensive, energy-consuming, and have low production yield [11].

Adsorption has been recognized as a promising technique for the removal of pollutants, including heavy metals, dyes, and many organic contaminants from aqueous solution. Adsorption is preferred over other conventional purification techniques due to its ease of operation, simplicity of design, high efficiency, and comparable low cost of application [12]. It can also be an alternative procedure for pre-treatment of WCO by offering a low-cost and straightforward FFA removal technique that reduces oil loss and soap contamination [13]. A variety of low-cost adsorbents derived from natural and agricultural wastes have demonstrated the capability for the removal of FFA. For example, Rengga at al. studied the FFA removal from WCO by the adsorbent derived from banana peel. The results showed that the maximum adsorption capacity (q_m) of the adsorbent ranged from 23.18-27.40 mg/g [14]. Chairgulprasert and Madlah developed the adsorbent from coffee husk and found the q_m of 2,000 mg/g [15]. Arahman et al. investigated the FFA removal from WCO by Java plum leaves and Guava fruits. The results showed that the q_m of Java plum leaves and Guava fruits was 141.99 and 133.77 mg/g, respectively [16]. Farook and Ravendran modified rice hull ash by using 14 M HNO_3 and studied its q_m for

†To whom correspondence should be addressed.
E-mail: amnatp@nu.ac.th

FFA adsorption. The results showed that the q_m of acid-modified rice hull ash ranged from 68.80-118.20 mg/g, depending on the length of FFA [17]. Baptiste et al. reported the q_m of −7.84 mg/g for FFA removal of acid-activated smectite clay [18]. The capability of the synthetic adsorbent for FFA adsorption was also reported. Ushedo at al. synthesized N, N(1,3-phenylene)dimethanimine for the removal of FFA from WCO and found that the q_m was 42.37 mg/g [19]. In addition, several studies demonstrated the adsorption of FFA capability of the adsorbents such as zeolite [20], montmorillonite [21], coal ash [13], pineapple dregs, and coconut husk [22]. Unfortunately, their q_m was not reported.

Cassava (*Manihot esculenta* Crantz) is considered one of Thailand's most important economic crops. A total area of 1.1 million hectares is devoted to cassava planting by many farmers, producing more than 31 million tons of roots annually [23]. Currently, 104 modern starch factories are operating in Thailand, with a total starch production of 15-17 million tons annually [24]. Several tons of cassava peels are generated from the processing activity. With limited utilization, cassava peels are usually discarded after harvesting and processing [25]. Improper disposal of cassava peels contributes largely to environmental problems. Several studies have tried converting cassava peels into value-added products to reduce environmental pollution, such as biomass, proteins source, livestock feed, and nanofibers [25-27].

Cassava peel comprises cellulose (40.5%), lignin (11.7%), and hemicellulose (21.4%) [27]. Cellulose consists of linear chains of glucose units linked by β-1,4-glycosidic bonds. It has the characteristic physicochemical property of having strong adsorption power, thereby making it a suitable adsorbent [28]. Therefore, with its high cellulose content, cassava peel has been considered as a potential adsorbent for removal of contaminants. Cassava peel has also been studied for adsorption heavy metal and dye from wastewater [29,30]. However, no study to date has examined the potential use of cassava as an adsorbent for FFA adsorption. In the present work, we prepared the adsorbent from cassava peel and investigated the surface morphology and functional groups of the adsorbent. The cassava-derived adsorbent was studied for the adsorption of FFA from WCO. The adsorption parameters such as adsorbent dosage, contact time, and temperature were analyzed. The kinetics, isotherm, and thermodynamics of FFA adsorption were investigated. In addition, the chemical regeneration of adsorbent was demonstrated.

MATERIALS AND METHODS

1. Waste Cooking Oil, Cassava Peels, and Chemicals

Fresh cooking oil was bought from the local supermarket in Phitsanulok, Thailand. Waste cooking oil (WCO) was prepared following Chairgulprasert and Madlah [15]. The % polar compounds and FFA content of WCO sample were determined before and after adsorption, as described in sections 2-4 and 2-6. Cassava peels were given generously from the cassava starch factory in Kamphaeng Phet, Thailand. Sodium hydroxide and phenolphthalein were purchased from Merck Co., Ltd. Sulfuric acid, methanol, diethyl ether, chloroform, and hexane were purchased from RCI Labscan Co., Ltd. All chemicals used were analytical grade. Polar Blue Test kit was purchased from Master Lab Part., Ltd.

2. Preparation of the Adsorbents from Cassava Peels

Cassava peels were washed with distilled water to remove the dirt and dried using an oven, and then crushed with a blender to obtain a cassava peel powder. The calcination process was performed at 200 °C and 600 °C without nitrogen, following Chairgulprasert and Madlah [15] and Rahayu et al. [22]. Four adsorbents were developed from a cassava peel powder as follows: (i) A1, a cassava peel powder was calcined at 600 °C for 2 hours in a furnace; (ii) A2, a cassava peel powder was calcinated at 200 °C for 2 hours; (iii) A3, a cassava peel powder was calcinated at 200 °C for 2 hours, followed by activation with 1 N NaOH for 1 hour; (iv) A4, a cassava peel powder was calcinated at 200 °C for 2 hours, followed by activation with 1 N H_2SO_4 for 1 hour.

3. Batch Adsorption

Batch adsorption, which was used to screen an effective adsorbent, was conducted in a 250-mL Erlenmeyer flask. One gram of the adsorbent was added to 50 mL of WCO, and the suspension was then shaken at 35 °C, 200 rpm for 2 hours. After adsorption, the suspension was left at room temperature for precipitation. Then, the adsorbent was filtered out, and the % polar compound that remained in treated WCO was analyzed as described in 2-4. An untreated WCO was used as a control sample. We used activated carbon and cassava peel powder as control adsorbents in batch adsorption.

4. Determination of % Polar Compound

The % polar compound in WCO sample was determined using Polar Blue Test kit (Master Lab Part., Ltd.), following the manufacturer's protocol. Briefly, WCO sample was mixed thoroughly with polar blue reagent in 1 : 1 ratio. The mixture was incubated at room temperature for 1 minute. The % polar compound in WCO sample was determined based on the mixture's color as follows: Blue, the % polar compound in oil sample is less than 20%; Green, the % polar compound in oil sample is between 20-25%; Yellow, the % polar compound in oil sample is more than 25%. The most effective adsorbent for removal of polar compounds was chosen for further studies including characterization, isotherms, kinetics, thermodynamics, and desorption studies.

5. Characterization of an Effective Adsorbent

The adsorbent surface was examined using scanning electron microscopy (SEM). The surface functional groups were studied using Fourier transform infrared spectrometry (FT-IR). SEM and FT-IR analysis were performed at Science Lab Center, Faculty of Science, Naresuan University.

6. Determination of Free Fatty Acid (FFA)

The FFA content in WCO before and after adsorption was analyzed using titration, according to the AOAC Official Method 940.28 (AOAC, 2016). Two grams of oil sample were mixed with 30 mL of diethyl ether : ethanol (1 : 1). Subsequently, the mixture was added with 1% phenolphthalein and titrated with 0.1 M NaOH. The FFA content was calculated following Eq. (1) and expressed as the amount of KOH in mg to neutralize 1 g of oil (mg_{KOH}/g) [31].

$$\mathrm{FFA} = \frac{40\mathrm{VN}}{\mathrm{W}_{oil}} \tag{1}$$

where V is the volume of NaOH titrant used (mL). N is Normality of NaOH. W_{oil} is the weight of WCO sample (g).

7. Effect of Adsorbent Dose and Isotherm Studies

The most effective adsorbent for adsorption of polar compounds was chosen for studying adsorption isotherm, kinetic, and thermodynamic for FFA adsorption from WCO. Batch adsorption experiment was conducted to determine the effect of adsorbent dose, contact time, and temperature on FFA adsorption. We conducted batch adsorption in a 250-mL Erlenmeyer flask. To determine the effect of adsorbent dosage, 1-5 g of the adsorbent was added to 50 mL of WCO, and the suspension was then shaken at 35 °C, 200 rpm for 2 hours. Then, the suspension was left at room temperature for precipitation, and the adsorbent was filtered out. The FFA content in WCO before and after adsorption was determined as described above. The adsorption capacity (q_e) and FFA reduction efficiency (% E) were calculated following Chairgulprasert and Madlah [15], as shown in Eqs. (2) and (3), respectively.

$$q_e = \frac{(C_i - C_e) \times V}{W} \tag{2}$$

$$\% E = \frac{(C_i - C_e)}{C_i} \times 100 \tag{3}$$

where q_e is the amount of adsorbate absorbed by the adsorbent (mg/g), C_i is initial concentration of FFA in WCO (mg_{KOH}/g), C_e is the concentration of FFA in WCO after adsorption (mg_{KOH}/g), V is the volume of oil sample (mL), W is the weight of adsorbent (g). Langmuir, Freundlich, and Temkin isotherm models were used to describe the equilibrium between adsorbate and adsorbent.

8. Effect of Contact Time and Kinetic Studies

The effect of contact time on FFA adsorption was determined by adding 2 g of the adsorbent to 50 mL of WCO in 250-mL Erlenmeyer flask. The suspension was shaken at 35 °C, 200 rpm for 30-300 minutes, and was then left at room temperature for precipitation. The adsorbent was filtered out, and the FFA content in WCO before and after adsorption was determined as described above. The pseudo-first-order and pseudo-second-order models were used to describe the kinetics of FFA adsorption.

9. Thermodynamic of FFA Adsorption

Thermodynamic parameters of adsorbent for FFA adsorption were also determined. Batch adsorption was performed using 2 g of the adsorbent and 50 mL of WCO. Adsorption was conducted at 35 °C, 45 °C, and 55 °C, 200 rpm for 2 hours. The FFA content in WCO before and after adsorption was determined as described above. Thermodynamic parameters of change in Gibbs free energy (ΔG^o), enthalpy (ΔH^o), and entropy (ΔS^o) were determined.

10. Desorption Study

A desorption study of the adsorbent was performed following Ushedo et al. [19] with some modifications. Batch adsorption and desorption studies were conducted in a 250-mL Erlenmeyer flask. For adsorption, the adsorbent (2 g) was added to 50 mL of WCO, and the suspension was then shaken at 35 °C, 200 rpm for 2 hours. The FFA content in WCO before and after adsorption was determined as described in section 2.6. For desorption, the FFA-laden adsorbent was dried at room temperature for 48 hours. Solvents including diethyl ether, hexane, and chloroform : methanol (2 : 1, v/v) were tested. To determine the desorption efficiency (% D), the FFA-laden adsorbent was separately mixed with 50 mL of solvent. Desorption was performed at 35 °C, 200 rpm for 2 hours. The amount of FFA desorbed was determined as described in section 2.6. The % D was determined following Ushedo et al. [19] and Sandhu and Gu [32] as shown in Eq. (4).

$$\% D = \frac{C_d V_d}{(C_i - C_e) V_i} \times 100 \tag{4}$$

where C_d is the concentration of FFA in solvent after desorption (mg_{KOH}/g), V_d is the volume of solvent (mL), C_i is initial concentration of FFA in WCO (mg_{KOH}/g), C_e is the concentration of FFA in WCO after adsorption (mg_{KOH}/g), V_i is the volume of oil sample (mL).

RESULTS AND DISCUSSION

1. Screening of the Most Effective Adsorbent for Adsorption of Polar Compound in WCO

The amounts of toxic compounds in cooking oil increase as the number of frying cycles, the duration of frying, and temperature.

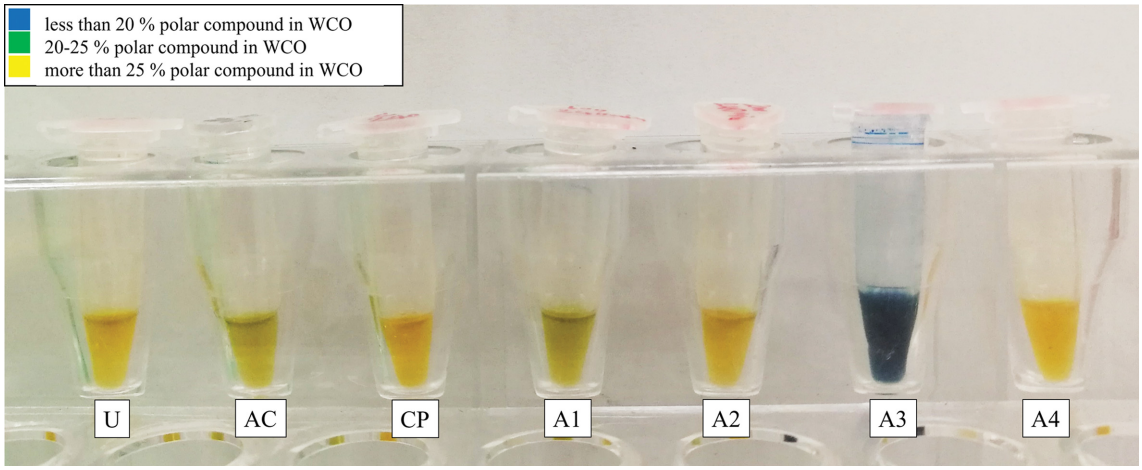

Fig. 1. Screening of the most effective adsorbent for removal of the polar compound in WCO. U is untreated WCO. AC, CP, A1, A2, A3, A4 are WCO treated using activated carbon, cassava peel powder, adsorbent A1, A2, A3, and A4, respectively.

When the polar compound in cooking oil exceeds 25% (w/w), it is no longer possible to use the oil in frying, and the oil should be discarded as WCO [33]. We developed four adsorbents and screened the most effective one for removal of the polar compound in WCO using batch adsorption. The results of the screening are shown in Fig. 1. By using the Polar Blue test kit (Master Lab), we found that the reaction which contained untreated WCO (U) was yellow, indicating that the untreated WCO contained more than 25% (w/w) of polar compound. Similar results were observed in WCO treated with cassava peel powder (CP), A2, and A4, indicating that A2 and A4 could not adsorb polar compound in WCO. WCO treated by activated carbon (AC) and A1 turned from yellow to green, indicating that the polar compound in WCO was 20-25% (w/w). This suggested that AC and A1 could slightly adsorb polar compounds in WCO. WCO treated by A3 was blue, indicating that the polar compound that remained in WCO was less than 20% (w/w). This suggested that A3 was the most effective adsorbent for removal of the polar compound in WCO.

2. Characterization of the Most Effective Adsorbent

Surface morphology of CP (Fig. 2(a)) and A1 (Fig. 2(b)) showed a rough surface with small granules, and porous structure was not observed. SEM images show that a significant change in morphology was observed after treatment with NaOH. SEM of A3 (Fig. 2(c)) showed the folded and porous structure, which may provide a large surface area to interact with polar compound in WCO. In addition, the SEM image at 1000X magnification of A3 showed the presence of the microhairy structure on the surface of the adsorbent (Fig. 2(d)). It has been demonstrated that NaOH treatment helps to remove the contaminants as well as increase the roughness and porousness of the adsorbent, increasing the adsorption efficiency [34]. Therefore, morphological changes of A3 may affect the efficiency in removal of the polar compound in WCO.

We analyzed the surface functional groups of the adsorbents using FT-IR. Fig. 3 shows FT-IR spectra of cassava peel powder, A1, and A3. Typical functional groups found in plant materials were detected in all three adsorbents. A strong, broad peak at 3,271-3,287 cm^{-1} was assigned to the O-H stretching vibration in alcohols, phenols, and carboxylic acids, typically found in pectin, cellulose, hemicellulose, and lignin. The functional groups, such as the carboxyl group and hydroxyl group, are typically found in biological adsorption material [35]. The peak at 2,916-2,927 cm^{-1} was C-H stretching vibration of aliphatic acids. The C=C stretching was identified at

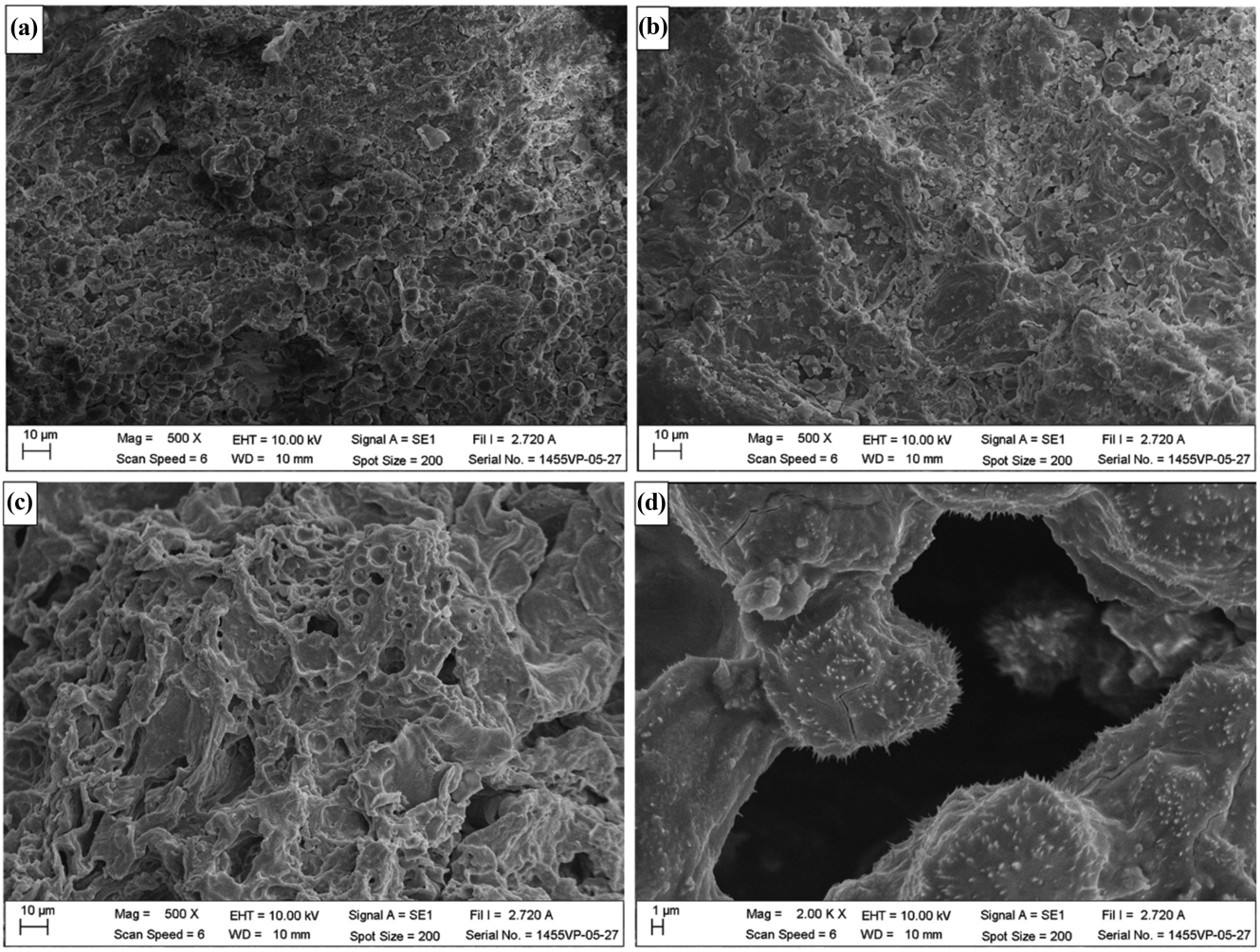

Fig. 2. Micrographs obtained by SEM of cassava peel powder ((a); 500x zoom), A1 ((b); 500x zoom), A3 ((c); 500x zoom), and A3 ((d); 2000x zoom).

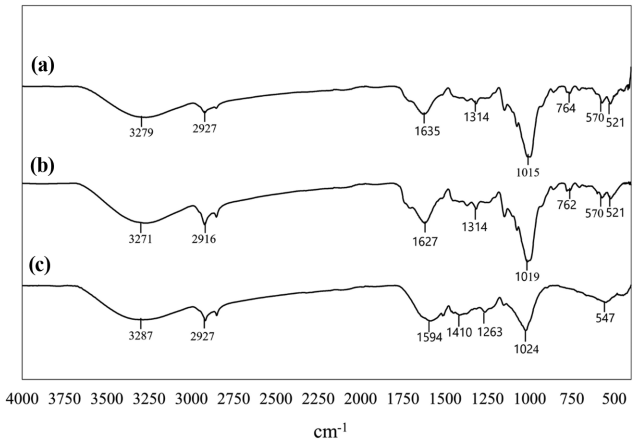

Fig. 3. FT-IR spectra of cassava peel powder (a), A1 (b), and A3 (c).

1,594-1,635 cm^{-1}, and the C-O stretching was identified at 1,015-1,024 cm^{-1}. A change of FT-IR spectra in the fingerprint region (400-1,500 cm^{-1}) was observed in A3 compared to CP and A1. NaOH may cause the modification of the surface functional groups. In addition, it can clean the surfaces, consequently revealing functional groups of adsorbent, especially the oxygen-containing functional groups [36], which might increase A3 adsorption capacity. Kumar and Bandyopadhyay reported that NaOH modification resulted in increasing the Cd(II) uptake of rice husk from 75% to 97%. In addition, the Cd(II) adsorption capacity of rice husk increased from 8.58 mg/g to 20.24 mg/g after NaOH modification [37].

3. Effect of Adsorbent Dose on FFA Adsorption

Adsorbent dose is an important parameter that significantly affects adsorption efficiency (% E) and adsorption capacity (q_e, mg/g) of the adsorbent. Therefore, the influence of A3 dose on FFA adsorption was investigated in the range of 1-5 g. The initial FFA content in WCO was 14.58 mg_{KOH}/g. After batch adsorption, the % E increased from 50.27% to 97.25% as the A3 dose increased from 1 to 5 g (Fig. 4(a)). The increase in % E with the A3 dose could be due to an increase in the adsorbent surface area, providing the number of adsorption sites available for adsorption, as already reported by many studies. Conversely, as the A3 dose was increased, the q_e decreased. This might be due to surplus amounts of adsorbents. Moreover, the decrease in q_e with increasing adsorbent dose might be due to aggregation. Aggregation of adsorbent leads to a decrease in total surface area of the adsorbent and increase in diffusional path length [38]. By using 2 g of A3 and the contact time of 2 hours, the amount of FFA being adsorbed by A3 reached a satisfactory level of 80.59 % E (Fig. 4(a)). With this data, the A3 dose was fixed at 2 g in the following experiments to prevent the aggregation of adsorbent.

4. Isotherm of FFA Adsorption

Langmuir, Freundlich, and Temkin isotherm models are most frequently used to represent the data of adsorption from solution. The Langmuir isotherm is a model for monolayer adsorption on a homogeneous surface [39]. The linear equation of Langmuir iso-

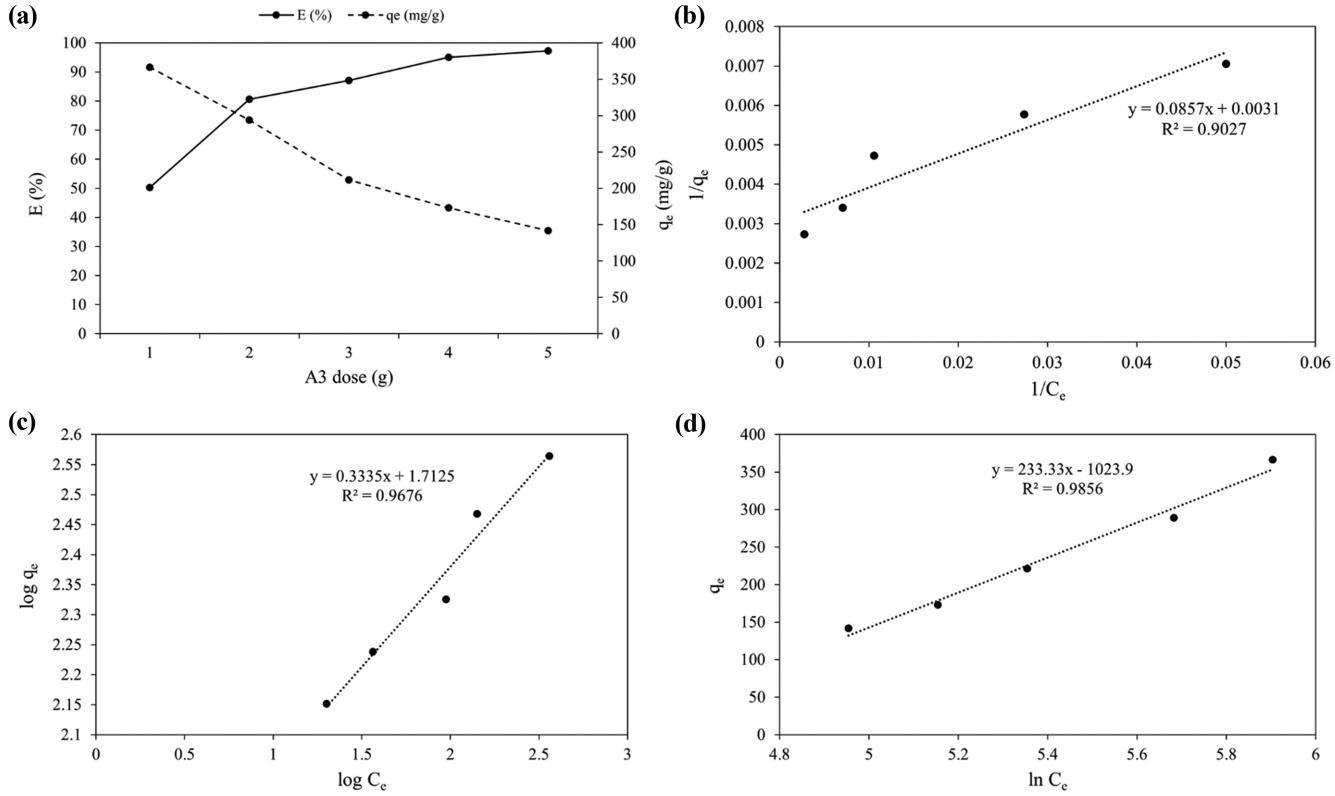

Fig. 4. Effect of A3 dose on FFA removal. (a) adsorption efficiency (E, %) and adsorption capacity (q_e) of A3 for FFA; (b) Langmuir, (c) Freundlich, and (d) Temkin isotherm plots of A3 for FFA adsorption (2 hours contact time, 35 °C).

therm is shown in Eq. (5).

$$\frac{C_e}{q_e} = \frac{1}{q_m K_L} + \frac{C_e}{q_m} \quad (5)$$

where C_e (mg/mL) is the equilibrium concentration of FFA in WCO, q_e (mg/g) is the amount of FFA adsorbed per unit mass of adsorbent, q_m (mg/g) is the maximum adsorption capacity, K_L is the adsorption equilibrium constant. The linear regression plot of $1/C_e$ versus $1/q_e$ of Langmuir isotherm is shown in Fig. 4(b). The slope and intercept determined the value of q_m and K_L, where q_m is 1/intercept, and K_L=1/slope q_m.

The Freundlich isotherm is based on a multilayer adsorption on a heterogeneous surface [40]. The linearized equation is shown in Eq. (6).

$$\log q_e = \log K_F + \left(\frac{1}{n}\right)\log C_e \quad (6)$$

where K_F is the Freundlich constant related to adsorption capacity; n is the adsorption intensity. The value of n and K_F can be determined from the slope and the intercept of the plotting of $\log C_e$ versus $\log q_e$ (Fig. 4(c)).

The Temkin isotherm is based on the assumption that the interaction of adsorbate and adsorbent occurred during surface coverage, resulting in a linear decrease in the heat of adsorption [41]. The linearized equation in shown in Eqs. (7) and (8).

$$q_e = (RT/b)\ln(K_T C_e) \quad (7)$$

$$q_e = B_T \ln K_T + B_T \ln C_e \quad (8)$$

where T (K) is the absolute temperature, R (J/mol·K) is the gas constant, K_T (L/mg) is the equilibrium binding constant, b (kJ/mol) is the variation of adsorption energy, and B_T (kJ/mol) is the Temkin constant, corresponding to the heat of adsorption. The value of b and K_T can be calculated from the slope of the plotting of $\ln C_e$ versus q_e (Fig. 4(d)). The values of B_T can be calculated from RT/b.

All the isotherm constants and correlation coefficients (R^2) are given in Table 1. The maximum adsorption capacity (q_m) of A3 was found to be 322.58 mg/g for FFA by using the Langmuir model equation. We compared the q_m of A3 for FFA with the q_m of other adsorbents in the literature, and the comparative data are given in Table 2. In most cases, the q_m of A3 was found to be better than the other adsorbents reported in the literature, except coffee husk [14-19]. The parameter R_L indicates the shape of the isotherm to be either unfavorable (R_L>1), linear (R_L=1), favorable (0<R_L<1), or irreversible (R_L=0) [42]. In our experiments, the value of R_L was 0.6542, suggesting that the adsorption of FFA on the surface of A3 was favorable. The Freundlich isotherm constant, n, represents the adsorption intensity. The value of 1/n gives an idea for the favorability of the adsorption process. If 1/n is greater than zero (0<1/n<1), the adsorption is favorable, if 1/n is greater than 1, the adsorption process is unfavorable, while it is irreversible when 1/n=1 [42]. We found that the value of 1/n of A3 was 0.3335, confirming that the adsorption of FFA onto A3 surface is a favorable process. By evaluating the Temkin isotherm, the heat of adsorption process (B_T) of A3 was 10.99 kJ/mol. The value of B_T gives information about the mechanisms of the adsorption process. If B_T value lies between 8 and 16 kJ/mol, the adsorption process takes place chemically, whereas when B_T<8 kJ/mol, the adsorption process proceeds physically [43]. Our result suggests that the FFA adsorption process of A3 is chemical adsorption.

Table 1. Isotherm constants and correlation coefficients (R^2) of FFA adsorption onto A3

Isotherm	Parameters	Values
Langmuir	q_m (mg/g)	322.582
	K_L (L/mg)	0.0362
	R_L	0.6542
	R^2	0.9027
Freundlich	K_F (mg/g)	51.5822
	1/n	0.3335
	R^2	0.9676
Temkin	B_T	10.9990
	b (J/mol)	233.3330
	K_T (L/mg)	0.0142
	R^2	0.9856

Table 2. Comparison of adsorption capacities (q_m) of FFA with some agricultural byproduct and synthetic adsorbent

Adsorbents	q_m (mg/g)	References
NaOH-activated cassava peel (A3)	322.58	This study
1 M HNO_3-modified rice hull	39.90-76.00	17
14 M HNO_3-modified rice hull	68.80-118.20	17
Banana peel (calcinated at 600 °C)	23.18	14
Banana peel (calcinated at 650 °C)	25.22	14
Banana peel (calcinated at 700 °C)	27.40	14
Coffee husk	2,000.00	15
Java plum leaves	141.99	16
Guava fruits	133.77	16
Acid-activated smectite	−7.85	18
N, N(1,3-phenylene)dimethanimine	42.37	19

By comparing the correlation coefficient values (R^2) obtained from three isotherm models, we found that the equilibrium data fitted well to Freundlich (R^2=0.9676) and Temkin models (R^2=0.9856). However, it has been reported that the Temkin isotherm model is inappropriate to present complex adsorption systems, including aqueous phase adsorption isotherm [44]. Therefore, we concluded that the Freundlich model best represents the experimental data and is best suited for the present work. Thus, the FFA adsorption onto A3 is multilayered adsorption onto a heterogeneous surface.

5. Effect of Contact Time on FFA Adsorption

The effect of contact time and adsorption kinetic was examined using 2 g of A3 in 50 mL of WCO. As shown in Fig. 5(a), the quantity of FFA in WCO decreased upon contact time. The FFA adsorption of A3 occurred rapidly at 30-120 minutes. The fast adsorption rate is due to the large amount of surface area available for adsorption of FFA. At higher contact time the rate of adsorption decreases, gradually leading to equilibrium. This decline is due to decrease in total adsorbent surface area and fewer available binding sites [45]. After the equilibrium period, the amount of FFA ad-

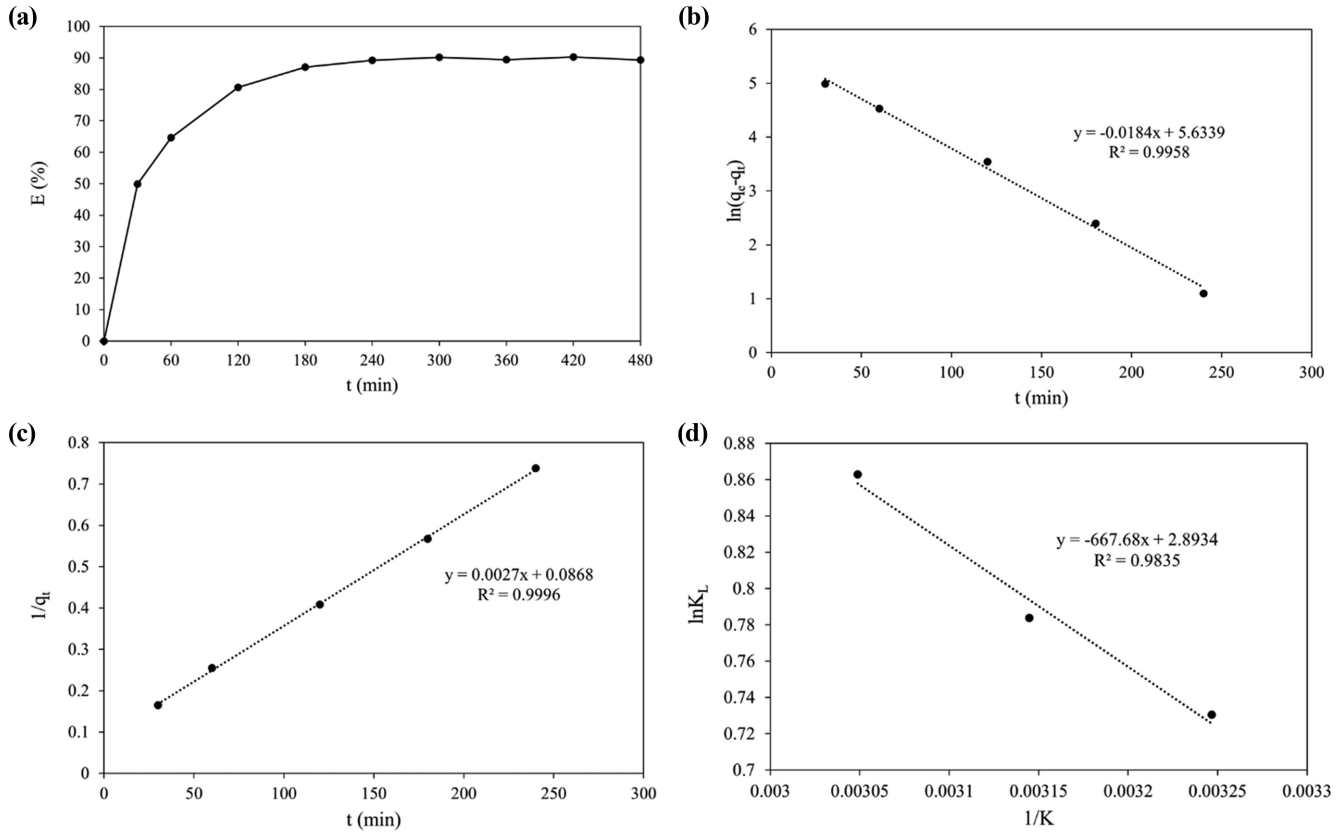

Fig. 5. Effect of contact time and temperature on FFA adsorption of A3. (a) FFA adsorption efficiency (E, %) of A3 at various time; (b) Pseudo-first-order plot of A3 for FFA adsorption (2 g dose, 35 °C); (c) Pseudo-second-order plot of A3 for FFA adsorption (2 g dose, 35 °C); (D) Thermodynamic plot for FFA adsorption of A3 (2 g dose, 2 hours contact time).

sorbed does not show time-dependent change. Similar results have been observed in literature for adsorption of FFA onto coffee husk ash [15]. The contact time of 120 minutes was used for further studies because the amount of FFA being adsorbed by A3 reached a satisfactory level (80.59% E).

6. Kinetics of FFA Adsorption

The kinetics of FFA adsorption was studied using pseudo-first order and pseudo-second order models [46] as shown in Eqs. (9) and (10).

$$\log(q_e - q_t) = \log q_e - \frac{k_1 t}{2.30} \tag{9}$$

$$\frac{t}{q_t} = \frac{1}{k_2 q_{e2}} + \frac{t}{q_e} \tag{10}$$

where q_t and q_e (mg/g) are the quantities of FFA adsorbed onto A3 at time (t, min) and at equilibrium time, respectively. The k_1 and k_2 are the first- and second-order rate constants. The linear regression plot of t versus $\ln(q_e - q_t)$ of the pseudo-first-order model is shown in Fig. 5(b). The linear regression plot of t versus t/q_t of the pseudo-second-order model is shown in Fig. 5(c).

The kinetic parameters of pseudo-first order and pseudo-second order models are shown in Table 3. Even though both kinetic models show high correlation coefficient (R^2) at 0.99, the kinetic data exhibits an excellent compliance with pseudo-second-order kinetic equation. As seen in Table 3, the calculated q_e values from pseudo-second-order model were closer to experimental q_e values than the pseudo-first-order model. The correlation for the system provided by the pseudo-second-order model suggests that the mechanism of FFA adsorption onto A3 surface occurred in a chemisorption manner, confirming the result of the Temkin isotherm model.

Table 3. Kinetic parameters and correlation coefficients (R^2) of FFA adsorption onto A3

Model	Parameters	Values
Experiment	q_e (mg/g)	328.25
Pseudo-first-order	q_e (mg/g)	279.75
	k_1 (1/min)	−7.66667E-05
	R^2	0.9958
Pseudo-second-order	q_e (mg/g)	370.37
	k_2 (g/(mg·min))	8.39862E-05
	R^2	0.9996

7. Thermodynamic of FFA Adsorption

The thermodynamics of FFA adsorption was examined using 2 g of adsorbent A3 in 50 mL of WCO. Batch adsorption was performed at 35, 45, and 55 °C for 2 hours. Thermodynamic parameters, including change in Gibbs free energy (ΔG^o), enthalpy (ΔH^o), and (ΔS^o) were determined following Eqs. (11) and (12) [15].

Table 4. Thermodynamic parameters and correlation coefficients (R^2) of FFA adsorption onto A3

Parameters	Values
ΔG^o (kJ/mol) at 35 °C (308 K)	−1.8704
ΔG^o (kJ/mol) at 45 °C (318 K)	−2.0725
ΔG^o (kJ/mol) at 55 °C (328 K)	−2.3532
ΔH^o (kJ/mol)	5.5511
ΔS^o (J/mol K)	24.0557
R^2	0.9835

$$\log\frac{q_e}{C_e} = \frac{\Delta S^o}{2.303R} - \frac{\Delta H^o}{2.303RT} \quad (11)$$

$$\Delta G^o = \Delta H^o - T\Delta S^o \quad (12)$$

where R is the gas constant (8.314 J/mol·K). The plot between $\log q_e/C_e$ versus T (K) is shown in Fig. 5(d). The values of ΔH^o and ΔS^o were calculated from the slope and the intercept, respectively. ΔG^o was calculated based on Eq. (11). Thermodynamic parameters are shown in Table 4.

As shown in Table 4, the FFA adsorption occurred with negative values for ΔG^o at all temperatures, suggesting that the FFA adsorption onto adsorbent A3 was a favorable and spontaneous process. The value of ΔG^o decreased with the increasing temperature, suggesting that higher temperature makes FFA adsorption easier. The positive values of ΔH^o indicated that the FFA adsorption onto adsorbent A3 is endothermic, which is supported by the increase of adsorption of FFA with a rise in temperature. The positive ΔS^o value indicated that the randomness increased at the liquid-solid interfaces during the adsorption of FFA onto adsorbent A3. Our results are contrary to previous studies on coffee husk ash. The FFA adsorption onto coffee husk ash was previously demonstrated as an exothermic process and increase of temperature resulted in increase of ΔG^o [15].

8. FFA Adsorption Mechanism of A3

Though it is complicated to understand the adsorption mechanism of FFA on A3, it is crucial. Two important factors which influence the chemical interactions of adsorbate and adsorbent are the structure of the adsorbate and the surface properties of the adsorbent [47]. In this study, kinetic data indicated that the FFA adsorption of A3 is a chemical adsorption; therefore, we hypothesize that the adsorption of FFA onto A3 surface might occur via chemical bonding. Fatty acids are molecules with a carboxylate COO- or COOH hydrophilic head, which is covalently linked to a hydrophobic tail of a hydrocarbon chain. The results of FT-IR put forward that NaOH treatment changes the A3 surface functional groups, and probably exposes the oxygen-containing functional groups such as hydroxyl group (-OH) to the A3 surface. This possibly will favor hydrogen-bonding between the more exposed hydroxyl groups (-OH) of A3 and the hydrophilic head (COO-) of FFA, while the hydrophobic tails of FFA may absorb onto the less polar surrounding groups on the A3 surface. In addition, NaOH treatment increases the roughness and porousness of A3. This possibly will favor mechanical bonding because FFA could penetrate more easily into A3 microstructure.

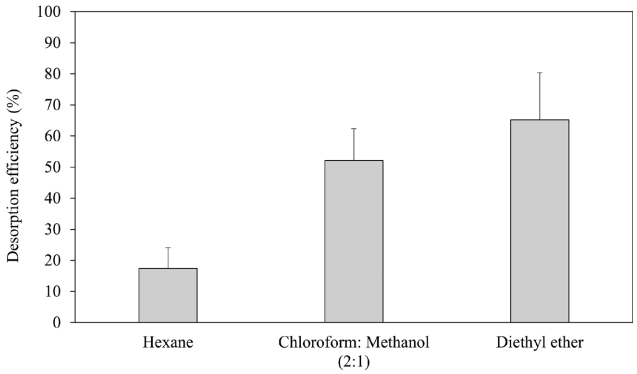

Fig. 6. FFA desorption capacity of A3 using different solvents.

9. Desorption of FFA

In the adsorption process, after all adsorption sites of adsorbent are fully occupied by adsorbates, the adsorption reaches equilibrium. Thereafter, adsorbent becomes totally inactive and is referred to as exhausted, spent or used adsorbent. This spent adsorbent is the main disadvantage of this process, as it is considered as a solid hazardous waste [36]. To overcome this problem, the regeneration of the spent adsorbent has been concerned. In this study, the desorption of FFA was studied to evaluate the regeneration of A3. Solvents such as hexane, diethyl ether, and chloroform : methanol (2 : 1, v/v) were tested for desorption of FFA from A3 surface. The results in Fig. 6 show that the % D of 65.21 and 52.17% was obtained using diethyl ether and chloroform : methanol (2 : 1), respectively, while hexane showed only 17.39% D. Our results are in line with Ushedo et al. [19]. Diethyl ether is often the preferred solvent as it is relatively non-polar and extracts most non-polar components. It was used in the AOAC official method 920.39 for lipid extraction [48]. Chloroform : methanol (2 : 1, v/v) is a biphasic mixture which has been reported by many studies as the effective solvent for lipid extraction [49]. Pati et al. reported that methanol can disrupt the hydrogen bonding between molecules [50]. Therefore, it might disrupt the hydrogen bonds between the hydroxyl groups (-OH) on A3 surface and the hydrophilic head (COO-) of FFA, dissociating FFA from active sites of A3. In addition, it has been reported that chloroform predominantly increases the solubility and diffusion of lipids [49]. Our results demonstrated that diethyl ether and chloroform : methanol (2 : 1, v/v) can be used for desorption of FFA, providing available active sites of A3 for the next round of adsorption. However, in this study, the partial regeneration of A3 was observed, as we obtained only 65.21 and 52.17% D by using diethyl ether and chloroform : methanol (2 : 1, v/v), respectively. Therefore, optimization of the condition for FFA desorption might be required.

Long-term stability of an adsorbent refers to its ability to maintain its adsorption properties over the number of adsorption-desorption cycles without significant loss of adsorption capacity. Long-term stability is a crucial factor as it determines adsorbent lifetime and operational costs of adsorption process [51]. Several factors can impact the long-term stability of an adsorbent. For example, high temperatures and humidity in the adsorption process can lead to physical and chemical degradation of the adsorbent, reducing its

adsorption capacity over time [52]. Similarly, exposure to corrosive chemicals during the adsorption-desorption cycle can cause chemical reactions that lead to degradation of the adsorbent and loss of adsorption capacity [53]. Contaminants present in the sample being treated can also negatively impact the stability of the adsorbent [54]. Finally, the method used for regeneration of the adsorbent can also have an impact on its long-term stability. For example, a harsh regeneration method such as boiling or microwaving can lead to physical and chemical degradation of the adsorbent, reducing its adsorption capacity [36]. For our study, the long-term stability of A3 for FFA adsorption should be further investigated before implementation.

CONCLUSION

Four cassava-derived adsorbents were developed by calcination at 600 °C and 200 °C with or without chemical modification. The adsorbent A3, which was developed by calcination at 200 °C, followed by NaOH modification, was found to be the most effective adsorbent for removal of polar compounds from WCO. FT-IR analysis revealed that the functional groups, such as the carboxyl group and hydroxyl group, are found on the surface of A3. Porous and microhairy structure of A3 was observed by using SEM analysis. The A3 was applied as an adsorbent for removal of FFA from WCO. The effect of adsorption parameters such as A3 dose, contact time, and temperature was studied using batch adsorption experiments. A satisfactory level of FFA adsorption of 80.59% E was observed by using 2 g of A3. Isotherms, kinetics and thermodynamics of A3 for FFA adsorption were also studied. The maximum adsorption capacity (q_m) of A3 for FFA was 322.58 mg/g at 35 °C. The FFA adsorption fit well to the Freundlich isotherm model. Based on Kinetic studies, the pseudo-second-order model provided the highest consistency with the experimental data, suggesting that the FFA adsorption of A3 was chemisorption. Thermodynamic study demonstrated that FFA adsorption onto adsorbent A3 was an endothermic, favorable, and spontaneous process. In addition, diethyl ether and chloroform : methanol (2 : 1, v/v) could be used for desorption of FFA from A3 surface. The obtained results demonstrated that A3 can be a suitable adsorbent for the removal of FFA from WCO. However, the optimal condition for desorption and long-term stability of A3 for FFA adsorption should be further investigated before implementation.

ACKNOWLEDGEMENTS

This research project is supported by Naresuan University (NU) and National Science, Research, and Innovation Fund (NSRF): Grant No. R2564B017. The authors would like to thank Assoc. Prof. Dr. Duangdao Channei (Department of Chemistry, Faculty of Sciences, Naresuan University) for technical support.

REFERENCES

1. M. R. Teixeira, R. Nogueira and L. M. Nunes, *Waste Manage.*, **78**, 611 (2018).
2. A. Orjuela and J. Clark, *Curr. Opin. Green Sustain. Chem.*, **26**, 100369 (2020).
3. V. Cordero-Ravelo and J. Schallenberg-Rodriguez, *J. Environ. Manage.*, **228**, 117 (2018).
4. D. C. Panadare and V. K. Rathod, *Iran. J. Chem. Chem. Eng.*, **12**, 55 (2015).
5. I. Thushari and S. Babel, *J. Environ. Manage.*, **310**, 114810 (2022).
6. E. Choe and D. B. Min, *J. Food Sci.*, **72**, R77 (2007).
7. D. Topi, *SN Appl. Sci.*, **2**, 513 (2020).
8. K. A. Zahan and M. Kano, *Energies*, **11**, 4 (2018).
9. Z.-Z. Cai, Y. Wang, Y.-L. Teng, K.-M. Chong, J.-W. Wang, J.-W. Zhang and D.-P. Yang, *Fuel Process. Technol.*, **137**, 186 (2015).
10. Y. Wang, S. Ma, L. Wang, S. Tang, W. W. Riley and M. J. T. Reaney, *Eur. J. Lipid Sci. Technol.*, **114**, 315 (2012).
11. R. Mićić, M. Tomić, F. Martinović, F. Kiss, M. Simikić and A. Aleksic, *Green Process. Synth.*, **8**, 15 (2019).
12. S. Karimi, M. Tavakkoli Yaraki and R. R. Karri, *Renew. Sust. Energ. Rev.*, **107**, 535 (2019).
13. E. Susilowati, A. Hasan and A. Syarif, *J. Phys. Conf. Ser.*, **1167**, 012035 (2019).
14. W. Rengga, A. Seubsai, S. Roddecha, A. Yudistira and A. Wiharto, *J. Phys. Conf. Ser.*, **1918**, 032008 (2021).
15. V. Chairgulprasert and P. Madlah, *Sci. Technol. Asia*, **23**, 1 (2018).
16. N. Arahman, R. A. Fitri, A. Wirakusuma, A. Fahrina and M. R. Bilad, *Int. J. Eng.*, **32**, 1372 (2019).
17. A. Farook and S. Ravendran, *J. Am. Oil Chem. Soc.*, **77**, 437 (2000).
18. B. M. Jean Baptiste, B. K. Daniele, E. Marie Charlène, T. T. Larrissa Canuala, E. Antoine and K. Richard, *Sci. Afr.*, **9**, e00498 (2020).
19. T. R. Ushedo, O. G. Adeyemi, A. Adewuyi and W. J. Lau, *Sci. Afr.*, **16**, e01188 (2022).
20. M. L. T. Ayu Putranti, S. K. Wirawan and I. M. Bendiyasa, *IOP Conf. Ser.: Mater. Sci. Eng.*, **299**, 012085 (2018).
21. B. M. Jean Baptiste, N. Esther, M. Praisler and R. Kamga, *Int. J. Biosci.*, **3**, 15 (2013).
22. S. Rahayu, Supriyatin and A. Bintari, *AIP Conf. Proc.*, **2019**, 050004 (2018).
23. A. I. Malik, P. Kongsil, V. A. Nguyễn, W. Ou, Sholihin, P. Srean, M. N. Sheela, L. A. Becerra López-Lavalle, Y. Utsumi, C. Lu, P. Kittipadakul, H. H. Nguyễn, H. Ceballos, T. H. Nguyễn, M. Selvaraj Gomez, P. Aiemnaka, R. Labarta, S. Chen, S. Amawan, S. Sok, L. Youabee, M. Seki, H. Tokunaga, W. Wang, K. Li, H. A. Nguyễn, V. Nguyễn, L. H. Hàm and M. Ishitani, *Breed. Sci.*, **70**, 145 (2020).
24. C. Sowcharoensuk, https://www.krungsri.com/en/research/industry/industry-outlook/agriculture/cassava/io/io-cassava-21 (accessed 5/2/2023 2023).
25. K. M. Oghenejoboh, H. O. Orugba, U. M. Oghenejoboh and S. E. Agarry, *Environ. Challenges*, **4**, 100127 (2021).
26. P. C. Jiwuba, L. C. Jiwuba, I. P. Ogbuewu and C. A. Mbajiorgu, *Trop. Anim. Health Prod.*, **53**, 207 (2021).
27. S. Widiarto, E. Pramono, Suharso, A. Rochliadi and I. M. Arcana, *Fibers*, **7**, 5 (2019).
28. Y. He, A. M. Dietrich, Q. Jin, T. Lin, D. Yu and H. Huang, *Food Bioprod. Process*, **135**, 227 (2022).
29. S. Rajeshwarisivaraj, S. Sivakumar, P. Senthilkumar and V. Subburam, *Bioresour. Technol.*, **80**, 233 (2001).
30. D. Schwantes, A. C. Gonçalves, G. F. Coelho, M. A. Campagnolo, D. C. Dragunski, C. R. T. Tarley, A. J. Miola and E. A. V. Leismann,

J. Chem., **2016**, 3694174 (2016).
31. L. Diaz and A. Brito, in *Prime archives in chemical engineering*, Vide Leaf, Hyderbad, India (2020).
32. A. K. Sandhu and L. Gu, *J. Agric. Food Chem.*, **61**, 1441 (2013).
33. S. Turan and A. Yalcuk, *J. Am. Oil Chem. Soc.*, **90**, 1761 (2013).
34. S. M. Abegunde, K. S. Idowu, O. M. Adejuwon and T. Adeyemi-Adejolu, *Resources Environ. Sustain.*, **1**, 100001 (2020).
35. Y. Zhou, L. Zhang and Z. Cheng, *J. Mol. Liq.*, **212**, 739 (2015).
36. T. Alsawy, E. Rashad, M. El-Qelish and R. H. Mohammed, *NPJ Clean Water*, **5**, 29 (2022).
37. U. Kumar and M. Bandyopadhyay, *Bioresour. Technol.*, **97**, 104 (2006).
38. G. T. Tee, X. Y. Gok and W. F. Yong, *Environ. Res.*, **212**, 113248 (2022).
39. M. A. Al-Ghouti, M. A. M. Khraisheh, S. J. Allen and M. N. Ahmad, *J. Environ. Manage.*, **69**, 229 (2003).
40. X.-j. Chen, Y. Wang, L.-l. Liu, J.-f. Cui, M.-y. Gan, D. H. K. Shum and R. C. K. Chan, *Psychiatry Res.*, **226**, 14 (2015).
41. M. Vadi, A. Mansoorabad, M. Mohammadi and N. Rostami, *Asian J. Chem.*, **25**, 5467 (2013).
42. N. Ayawei, A. N. Ebelegi and D. Wankasi, *J. Chem.*, **2017**, 3039817 (2017).
43. A. Bazan-Wozniak, J. Cielecka-Piontek, A. Nosal-Wiercińska and R. Pietrzak, *Materials*, **15**, 8000 (2022).
44. M. A. Al-Ghouti and D. A. Da'ana, *J. Hazard. Mater.*, **393**, 122383 (2020).
45. P. Saha, S. Chowdhury, S. Gupta and I. Kumar, *Chem. Eng. J.*, **165**, 874 (2010).
46. W. Rudzinski and W. Plazinski, *Environ. Sci. Technol.*, **42**, 2470 (2008).
47. S. Chakraborty, S. Chowdhury and P. Das Saha, *Carbohydr. Polym.*, **86**, 1533 (2011).
48. N. J. Thiex, S. Anderson, B. Gildemeister and Collaborators, *J. AOAC Int.*, **86**, 888 (2003).
49. M. W. K. Wong, N. Braidy, R. Pickford, P. S. Sachdev and A. Poljak, *Front. Neurol.*, **10**, 879 (2019).
50. S. Pati, B. Nie, R. D. Arnold and B. S. Cummings, *Biomed. Chromatogr.*, **30**, 695 (2016).
51. M. Jahandar Lashaki, S. Khiavi and A. Sayari, *Chem. Soc. Rev.*, **48**, 3320 (2019).
52. P. G. Parzuchowski, A. Świderska, M. Roguszewska, K. Rolińska and D. Wołosz, *Energy Fuels*, **34**, 12822 (2020).
53. S. F. Azha and S. Ismail, *IOP Conf. Ser.: Mater. Sci. Eng.*, **796**, 012054 (2020).
54. G. Zhang, J. Zhang, J. Zeng, Y. Sun, Y. Shen, X. Li, X. Ren, C. Hai, Y. Zhou and W. Tang, *Colloids Surf. A Physicochem. Eng. Asp.*, **629**, 127465 (2021).